

FCI-QMC approach to the Fermi polaron

M. Kolodrubetz¹, B. K. Clark^{1,3}

¹*Department of Physics, Princeton University, Princeton, NJ 08544, USA. and*

³*Princeton Center for Theoretical Science, Princeton University, Princeton, NJ 08544, USA.*

(Dated: May 28, 2018)

Finding the ground state of a fermionic Hamiltonian using quantum Monte Carlo is a very difficult problem, due to the Fermi sign problem. While still scaling exponentially, full configuration-interaction Monte Carlo (FCI-QMC)¹ mitigates some of the exponential variance by allowing annihilation of noise – whenever two walkers arrive at the same configuration with opposite signs, they are removed from the simulation. While FCI-QMC has been quite successful for quantum chemistry problems^{1,2}, its application to problems in condensed systems has been limited^{3,4}. In this paper, we apply FCI-QMC to the Fermi polaron problem, which provides an ideal test-bed for improving the algorithm. In its simplest form, FCI-QMC is unstable for even a fairly small system sizes. However, with a series of algorithmic improvements, we are able to significantly increase its effectiveness. We modify fixed node QMC to work in these systems, introduce a well chosen importance sampled trial wave function, a partial node approximation, and a variant of released node. Finally, we develop a way to perform FCI-QMC directly in the thermodynamic limit

PACS numbers: 05.10.Ln

Full configuration-interaction quantum Monte Carlo (FCI-QMC)¹ is a method for finding the ground state of a fermionic Hamiltonian H . Starting from some state $|\psi_i\rangle$ with non-zero ground state overlap, FCI-QMC stochastically performs imaginary time propagation $|\psi_\beta\rangle = e^{-\beta H}|\psi_i\rangle$. Working in a second quantized formalism, where anti-symmetry enters in the off-diagonal components of H , FCI-QMC formally yields the fermionic ground state $|\psi_0\rangle$ for sufficiently large β .

The wavefunction at any instant in imaginary time is sampled as a set of N_w walkers, where each walker is a signed element of some many-body basis. Breaking up $e^{-\beta H}$ into N small time steps, $e^{-\beta H} = e^{-\beta H/N} e^{-\beta H/N} \dots e^{-\beta H/N} \approx (1 - \tau H)^N$, where $\tau = \beta/N$, one applies the operator $U_1 = 1 - \tau H$ stochastically⁵.

The fermion sign problem manifests in the negative off-diagonal elements of U_1 , whose sign is set by Fermi statistics⁶. In general, there will be loops such that a walker starts in some basis state $|D\rangle$, hops around the loop via the off-diagonal elements of U_1 , and then returns to $|D\rangle$ with the opposite sign. If these sign-violating loops exist for a given Hamiltonian and basis, they are said to have a sign problem.

FCI-QMC attempts to mitigate the sign problem by annihilation; any time two walkers end up on $|D\rangle$ with opposite signs, they are both removed from the simulation. It relies on efficient annihilation to prevent walkers with the incorrect sign from propagating as noise. In principle one can always pick a very large N_w to achieve efficient annihilation, but the necessary number of walkers increases significantly with basis size. The efficiency of FCI-QMC has been explored in a few systems, including all-electron molecules¹, the homogeneous electron gas³, and the Hubbard model⁴.

In this paper we develop extensions to FCI-QMC and apply these new developments to the Fermi polaron⁷. The polaron is a classic problem in condensed matter physics, as it is one of the simplest problems that shows strongly-interacting many body effects. We will be particularly interested in the Fermi polaron as seen in cold atomic gases⁸, whose ground state properties are well understood through a combination of analytical⁷ and numerical⁹ methods. As such, the polaron problem serves as a nice test-bed for testing and improving the FCI-QMC algorithm in a condensed matter setting.

In the remainder of this paper, we introduce the polaron problem and discuss how we calculate its properties by improving on the FCI-QMC algorithm. In particular, we develop approaches which start with a sign-free Hamiltonian and reintroduce these signs so as to achieve an exact answer. In addition, we develop a way to do FCI-QMC in the thermodynamic limit.

In section I, we introduce the polaron. Then, for a test value of 10^6 walkers, we find that the naive implementation of FCI-QMC works for a basis restricted to only a single excitation on the non-interacting ground state, but fails for cases with additional excitations. We proceed to describe a trial wavefunction (section III) inspired by variational solutions to the polaron problem¹⁰ and introduce a variant of FCI-QMC which performs importance sampling. This increases the accessible parameter regime, but not sufficiently. Next, we introduce a controlled approximation (section IV) to attenuate the sign problem, which we call the partial node approximation. We extrapolate observables deduced from partial node simulations to the exact answers. We then combine release node techniques (section V) with the partial node approximation as an alternative way to find the true ground state observables. The partial node energies, although extrapolable to the correct result, are not individually variational. At the cost of a time-step error, we show (section VI) how to recover the variational guarantee by performing a more typical fixed-node approach. To accomplish

this, we overcome the non-trivial obstacle that a single basis element is connected by the Hamiltonian to an extremely large number of other basis elements. We discover that all three approaches for computing the ground state properties are consistent with each other and in agreement with other analytical and numerical work (section VII). Finally, we note that extrapolation to the thermodynamic limit is made difficult by the presence of shell effects. To avoid shell effects, we introduce an extension of the FCI-QMC algorithm that allows for working directly in the thermodynamic limit (section VIII). We compare and contrast our thermodynamic limit solution with that of diagrammatic Monte Carlo, and comment on future possibilities for utilizing our improvements to FCI-QMC in the field of condensed matter physics.

I. THE POLARON PROBLEM

The polaron problem we consider is defined for a three-dimensional system of two fermion species, denoted spin up and spin down. Starting with a non-interacting Fermi sea of spin up particles, a single spin down “impurity” is added that is able to interact with the sea of spin ups. Experimentally, near a broad s-wave Feshbach resonance the fermions interact by a short-range potential with scattering length a . The momentum space Hamiltonian is⁷

$$H = \sum_{k\sigma} \epsilon_k c_{k\sigma}^\dagger c_{k\sigma} + \frac{g}{\mathcal{V}} \sum_{kpq} c_{k+q,\uparrow}^\dagger c_{p-q,\downarrow}^\dagger c_{p,\downarrow} c_{k,\uparrow}, \quad (1)$$

where $\epsilon_k = k^2/(2m)$, \mathcal{V} is the volume of the system, and m is the mass of the particles. We work in units where $\hbar = 1$.

We regularize the short-range interaction by introducing a high-momentum cutoff Λ on the spin-ups. The interaction strength g is cutoff-dependent¹¹:

$$g^{-1} = \frac{1}{8\pi a} - \frac{\Lambda}{4\pi^2}. \quad (2)$$

We solve this Hamiltonian for a cube of side length $L = \mathcal{V}^{1/3}$ with periodic boundary conditions. With N spin up particles, the Fermi wavevector and energy are $k_F = (6\pi^2 N/\mathcal{V})^{1/2}$ and $E_F = k_F^2/(2m)$ respectively.

In the non-interacting limit ($a = 0$), the ground state is an undressed polaron,

$$|D_0\rangle \equiv |\text{FS}_\uparrow, \mathbf{0}_\downarrow\rangle, \quad (3)$$

where $|\text{FS}_\uparrow, \mathbf{0}_\downarrow\rangle$ denotes a Fermi sea of spin-up particles with a single spin down at zero momentum. Upon turning on a weak attractive interaction (small negative a), the polaron remains a well-defined quasiparticle with non-zero quasiparticle residue $Z = |\langle\psi_0|D_0\rangle|^2$, where $|\psi_0\rangle$ is the ground state of the interacting Hamiltonian. Note that Z can be written as the ground state expectation $\langle\psi_0|\mathcal{P}_0|\psi_0\rangle$, where $\mathcal{P}_0 = |D_0\rangle\langle D_0|$ projects onto the undressed polaron.

The polaron problem has been most thoroughly investigated for the case where the scattering is unitary limited, $(k_F a)^{-1} = 0$. Chevy found that the ground state for these parameters is well-described by a variational wavefunction that includes all single particle-hole excitations on the spin up Fermi sea, giving a ground state energy of $-0.6066E_F$ ^{7,10}. These results were later extended by Combescot and Mora¹⁰, who introduced a procedure for calculating the variational ground state energy at an arbitrary number of particle-hole excitations and proceeded to solve for the two particle-hole pair variational energy, $-0.6156E_F$.

The Fermi polaron has also been approached via Monte Carlo techniques, most notably diagrammatic Monte Carlo⁹. Monte Carlo results for the ground state energy agree well with the variational solutions. Given the agreement of the ground state polaron energy between variational expansions, Monte Carlo, and experiment⁸, the energetics of the polaron at unitarity are a good test case for improvements to the FCI-QMC algorithm.

Off of unitarity on the BEC side ($a^{-1} > 0$), the polaron eventually becomes unstable to formation of a tightly-bound molecule. This is theoretically predicted to occur as a first order “phase transition”¹¹ near $(k_F a)^{-1} = 0.9$. However, experimentally the quasiparticle residue vanishes at $(k_F a)^{-1} \approx 0.75$ ⁸. It is believed that this difference is due to the small but finite density of the spin down particles in the experiment; we will address this issue in sec. VII.

II. FCI-QMC APPLIED TO THE POLARON

Given the effectiveness of the variational expansions in describing the polaron, we choose as our basis all momentum space determinants with at most M particle-hole pairs dressing the spin-up Fermi sea. The Chevy ansatz⁷ is then, for example, the exact solution for $M = 1$. In this basis, all off-diagonal elements of H come from the interaction and are given by the constant value g/\mathcal{V} , with their sign set by Fermi statistics. We fix the number of spin-up particles N

Λ	M	N	$1/(k_F a)$	α	β	Basis size
20	1	33	0	-0.6	20	1.09×10^6
20	2	33	0	-0.6	20	2.88×10^{11}
20	3	33	0	-0.6	20	3.28×10^{16}
20	4	33	0	-0.6	20	2.03×10^{21}
20	2	33	0.5	-1.22	29.6	2.88×10^{11}
20	2	33	0.9	-2.22	37.3	2.88×10^{11}
20	2	∞	0	-0.6	20	∞

TABLE I: Basis size and variational parameters α and β used for different Hamiltonians defined by $[\Lambda, M, N, 1/(k_F a)]$, as described in the text.

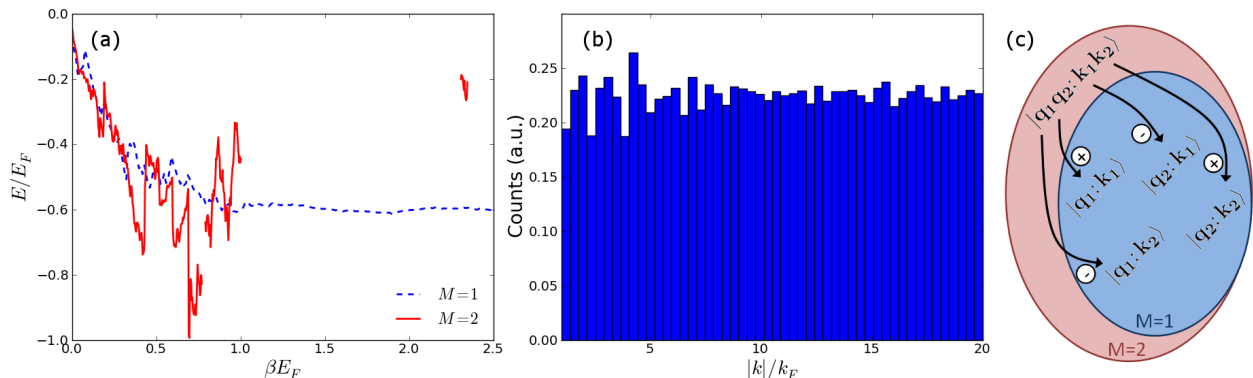


FIG. 1: (color online) (a) Polaron energy traces at $(k_F a)^{-1} = 0.9$ for importance sampled FCI-QMC with $N = 33$ spin up particles, momentum cutoff $\Lambda/k_F = 20$, $M = 1$ (dashed blue), and $M = 2$ (solid red). Discontinuities in the $M = 2$ data are regions where the denominator of the energy metric (5) passes through zero. (b) Histogram showing the momentum distribution of the particle excitations for the $M = 1$ data in part (a). Momenta are uniformly occupied from the edge of the Fermi sea ($k = k_F$) up to the cutoff ($k = 20k_F$). (c) Graphical representation of sign issues for the polaron. One can show that single particle-hole excitations all have positive signs in the exact ground state, but determinants with two particle-hole pairs are connected to them by signs that are half positive and half negative.

and momentum cutoff Λ . Note that we eventually want to take the physical limit $N \rightarrow \infty$ and $\Lambda \rightarrow \infty$, for which the basis size becomes infinite. We work in the sector with zero total momentum, which is always valid for a polaron-like quasiparticle¹¹. N will be limited to 7, 19, 27, ... to ensure that the spin up Fermi sea is a closed shell.

The walkers are initialized in the undressed polaron state with positive sign, $|\psi_i\rangle = |D_0\rangle$. Each walker is labeled by the pair $\{S_w, |D_w\rangle\}$, corresponding to its sign and determinant respectively. We will write general determinants as

$$|D\rangle = |\mathbf{k}_1, \mathbf{k}_2, \dots, \mathbf{k}_M; \mathbf{q}_1, \dots, \mathbf{q}_M\rangle = c_{\mathbf{k}_1}^\dagger \cdots c_{\mathbf{k}_M}^\dagger c_{\mathbf{q}_1} \cdots c_{\mathbf{q}_M} |D_0\rangle, \quad (4)$$

where \mathbf{k} 's label the particle excitations, \mathbf{q} 's label the holes, $\mathbf{k}_1 < \mathbf{k}_2 < \dots < \mathbf{k}_M$, and $\mathbf{q}_1 < \dots < \mathbf{q}_M$ for an arbitrary but fixed momentum ordering. The values of \mathbf{k}_i and \mathbf{q}_i are restricted to momenta on a discrete grid set by the size of the box. The energy metric in this basis is

$$E(\beta) = \frac{\langle D_0 | H | \psi_w(\beta) \rangle}{\langle D_0 | \psi_w(\beta) \rangle} = \frac{\sum_w S_w \langle D_0 | H | D_w \rangle}{\sum_w S_w \langle D_0 | D_w \rangle}, \quad (5)$$

where the zero of energy is defined as $\langle D_0 | H | D_0 \rangle = 0$. For sufficiently large β , the average of $E(\beta)$ converges to the fermionic ground state energy.

At unitarity with $N = 33$ and $\Lambda = 20$, FCI-QMC is able to find the ground state energy for $M = 1$, where the sign problem is weak (fig. 1a). For $M = 2$ however, the sign problem prevents convergence with fixed number of walkers $N_w = 10^6$ (fig. 1a). The $M = 2$ sign problem can be understood by starting from a determinant with two particle-hole pairs, $|D_2\rangle = |\mathbf{k}_1, \mathbf{k}_2; \mathbf{q}_1, \mathbf{q}_2\rangle$. Off-diagonal matrix elements allow hopping from $|D_2\rangle$ to four single particle-hole determinants (see fig. 1c). Of these, two come with positive sign, two with negative sign, and all have the same weight g/\mathcal{V} . So the determinants with two particle-hole pairs rain down nearly-random signs on the single particle-hole shell, which one can show should all be positive in the ground state. This results in a large sign problem unless the random signs are efficiently annihilated.

We emphasize that our approach to the Fermi polaron differs from previous problems where FCI-QMC has been applied because 1) we cut off the Hamiltonian after a fixed number of particle-hole pairs, 2) we have a single particle basis that is extremely large, and 3) almost all determinants are important. The last fact arises because the interaction is short-range in real space, i.e. long-range in momentum space. Fig. 1b shows a histogram of the walkers in the first particle-hole shell for the $M = 1$ ground state. The particle excitations are evenly occupied from the Fermi sea all the way up to the cutoff, in contrast to situations¹ where the ground state consists of a few large-weight determinants; this makes annihilation more difficult.

FCI-QMC for quantum chemistry problems minimizes these issues through an intelligent choice of single particle orbitals. However, for the Fermi polaron, there is no clear choice of basis that minimizes the impact of unimportant determinants. In the next section we show that using importance sampling can enhance the quality of the algorithm. This not only improves the variance, as usual in importance sampling, but also improves the annihilation properties by favoring certain determinants.

III. IMPORTANCE SAMPLING AND TRIAL WAVE-FUNCTION

Importance sampling is by now a standard Monte Carlo technique that has been used to decrease statistical noise. Importance sampling consists of sampling walker $|D\rangle$ from a probability distribution proportional to $|\langle D|\psi_T\rangle\langle D|\psi_0\rangle|$ instead of $|\langle D|\psi_0\rangle|$, where $|\psi_T\rangle$ is a trial wavefunction that we choose. This is implemented by re-weighting the off-diagonal moves, and can be thought of as simply acting with the (non-Hermitian) effective ‘‘Hamiltonian’’ H_{is} given by

$$\langle D'|H_{\text{is}}|D\rangle = \langle D'|H|D\rangle \frac{\langle \psi_T|D'\rangle}{\langle \psi_T|D\rangle}. \quad (6)$$

The energy metric becomes

$$E(\beta) = \frac{\sum_w S_w \langle D_0|H|D_w\rangle / \langle \psi_T|D_w\rangle}{\sum_w S_w \langle D_0|D_w\rangle / \langle \psi_T|D_w\rangle}. \quad (7)$$

We also calculate quasiparticle residue through the method of mixed estimators¹²,

$$Z \approx 2\langle \psi_T|\mathcal{P}_0|\psi_0\rangle - \langle \psi_T|\mathcal{P}_0|\psi_T\rangle. \quad (8)$$

As H_{is} is not Hermitian, we must be careful to only act with it on kets.

Choosing an appropriate trial wavefunction plays a major role in the success of importance sampling. A naive guess, the free fermion wavefunction, would give $|\psi_T\rangle = |D_0\rangle$; this would not allow sampling of any particle-hole excitations. Therefore, we must construct some $|\psi_T\rangle$, which in general we would like to be as close as possible to the ground state $|\psi_0\rangle$.

To motivate our choice of $|\psi_T\rangle$, consider the Schrödinger equation $H|\psi_0\rangle = E_0|\psi_0\rangle$. If $H = T + V$, where the kinetic term T is diagonal in the momentum basis, then

$$\langle D|\psi_0\rangle = -\frac{1}{\langle D|\hat{T}|D\rangle - E_0} \sum_{D'} \langle D|V|D'\rangle \langle D'|\psi_0\rangle. \quad (9)$$

For $|D\rangle$ with n particle-hole pairs, the interaction term connects it to determinants $|D'\rangle$ with $n - 1$, n , and $n + 1$ particle-hole pairs. The strength of the interaction is g/\mathcal{V} with sign $S_{D'} \equiv \text{sgn}(\langle D|V|D'\rangle)$. While these coupled linear equations are generally hard to solve, we can make the simplifying approximation of only considering $|D'\rangle$ with $n - 1$ particle-hole pairs in constructing $|\psi_T\rangle$. To allow some freedom, we will define variational coefficients α and β to replace g and E_0 respectively, giving

$$\langle D_n|\psi_T\rangle = -\frac{\beta/\mathcal{V}}{\langle D_n|\hat{T}|D_n\rangle - \alpha} \sum_{\substack{D'_{n-1} \text{ s.t.} \\ \langle D'_{n-1}|V|D_n\rangle \neq 0}} S_{D'_{n-1}} \langle D'_{n-1}|\psi_T\rangle, \quad (10)$$

where $|D_n\rangle$ denotes a determinant with n particle-hole pairs. This gives a recursive definition for $|\psi_T\rangle$ which, since normalization is irrelevant, we seed from $\langle D_0|\psi_T\rangle = 1$. The parameter α is chosen to be approximately the energy. Then, for each shell of n particle-hole pairs, we calculate $Z_n = \langle \psi_T|\mathcal{P}_n|\psi_T\rangle$ using variational Monte Carlo, where \mathcal{P}_n projects onto the subspace of determinants with n excitations. β is chosen to minimize the maximum deviation of Z_n from its average value, $1/(M + 1)$.

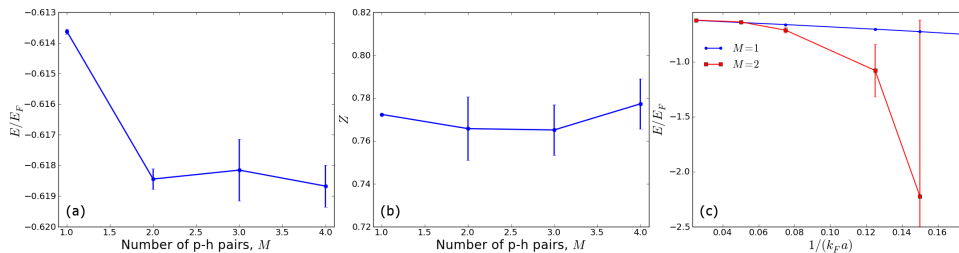


FIG. 2: (color online) Polaron energy (a) and quasiparticle residue (b) for $N = 33$, $(k_F a)^{-1} = 0$, $\Lambda/k_F = 20$, with $M = 1$ to 4 particle-hole excitations (to improve statistics we use $\gamma = 0$, so energies are a variational upper bound). Panel (c) shows energies upon breaking off of unitarity. Error bars are all computed for runs of fixed imaginary time $\Delta\beta = 35/E_F$ and therefore can be reasonably compared with each other. No data is shown for $(k_F a)^{-1} > 0.15$ with $M = 2$ because the simulation failed to converge a sign structure in that regime.

There is one minor issue with this ψ_T : due to the discreteness of the Hilbert space, eq. (10) will potentially yield $\langle D|\psi_T\rangle = 0$ for some small set of determinants $|D\rangle$, which become increasingly scarce as $N \rightarrow \infty$. This prevents any weight from being put on these determinants, introducing a bias. To avoid this bias, we introduce a third parameter γ such that if eq. (10) yields $|\langle D|\psi_T\rangle| < \gamma$, we set $\langle D|\psi_T\rangle \rightarrow \gamma$. The biased simulation $\gamma = 0$ gives a variational upper bound on the energy, which should be fairly close to correct. As an example, at unitarity for the relatively small basis with $N = 7$, $\Lambda = 10k_F$, and $M = 3$, the difference in energy is $-0.6279(3)E_F$ for $\gamma = 0$ versus $-0.6310(17)E_F$ for $\gamma = 10^{-4}$. We use $\gamma = 10^{-4}$ throughout the remainder of this paper, unless otherwise specified.

Importance sampling greatly improves the effectiveness of FCI-QMC. For example, at unitarity FCI-QMC with importance sampling is able to solve the polaron ground state for $\Lambda = 20k_F$, $N = 33$, and $M = 4$ – corresponding to a basis size of 2.03×10^{21} – using only 10^6 walkers. Solutions for the polaron energy and quasiparticle residue at unitarity are shown in fig. 2a,b.

We next push to positive values of a^{-1} , where for $(k_F a)^{-1} > 0.9$ the polaron is expected to become unstable to formation of a molecule. As the interaction strength $1/(k_F a)$ is increased, the polaron becomes more strongly correlated. The weight of the wavefunction is pushed to higher momenta, making annihilation more difficult. As seen in fig. 2c, for $M = 2$ particle-hole pairs, the error bar gradually increases as we push off of unitarity. Eventually, for $1/(k_F a) > 0.15$, FCI-QMC with importance sampling fails to find the ground state. To proceed, we now introduce modifications that allow us to further stabilize the algorithm.

IV. PARTIAL NODE APPROXIMATION

Fixed node quantum Monte Carlo is a method that removes the exponential cost of solving a fermionic Hamiltonian by approximating the Hamiltonian with a related one that has no sign problem. In this section we instead find a way to extrapolate to the exact solution of our (restricted basis) Hamiltonian using a fixed node-inspired starting point. In fixed node algorithms, such as the lattice formulation of van Bemmelen et al.¹³, one must specify a “correct” sign for each determinant. For simplicity we choose to use $|\psi_T\rangle$ as determining our sign structure. Given this choice, an off-diagonal element $\langle D'|H_{is}|D\rangle$ will be called sign-violating if $\langle D'|H_{is}|D\rangle > 0$, since in this case applying $-\tau H_{is}$ to hop from D to D' would flip the sign, violating the sign structure of $|\psi_T\rangle$.

The fixed node Hamiltonian H_{fn} is given by

$$\begin{aligned} \langle D'|H_{fn}|D\rangle &= \begin{cases} 0 & \text{if sign viol. (s.v.)} \\ \langle D'|H_{is}|D\rangle & \text{if not s.v. (n.s.v.)} \end{cases}, \text{ where } D \neq D' \\ \langle D|H_{fn}|D\rangle &= \langle D|H_{is}|D\rangle + \sum_{D' \text{ s.v.}} \langle D'|H_{is}|D\rangle. \end{aligned} \quad (11)$$

Note that the sign-violating off-diagonal matrix elements have been removed and “dumped” onto the diagonal. This H_{fn} is guaranteed to give a variational upper bound on the ground state energy, yielding the correct ground state energy if $|\psi_T\rangle = |\psi_0\rangle$.

Lattice fixed node was originally designed for real space lattices where there are very few off-diagonal elements connected to any given configuration. For our Hamiltonian, there will in general be many sign-violating matrix elements connected to a given determinant $|D\rangle$ (of order $> 10^7$ for our parameters), and the sums required to modify the diagonals of H_{fn} become analytically intractable. We therefore initially work with a modified Hamiltonian H'_{fn} –

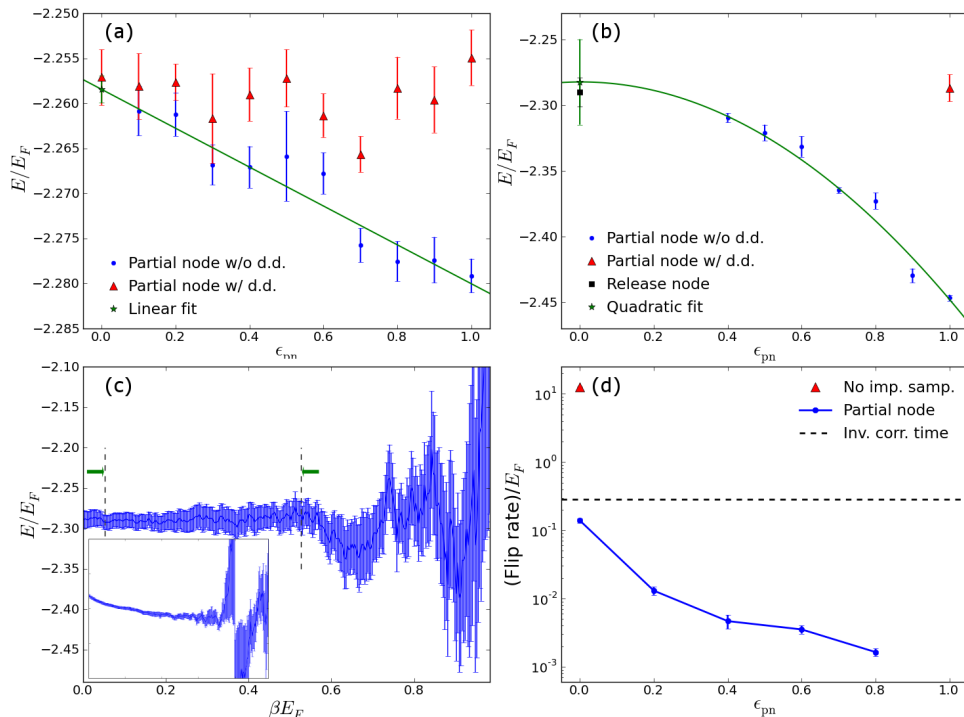


FIG. 3: (color online) (a) Partial node FCI-QMC energies, both with (red triangles) and without (blue dots) diagonal dumping (see text). Note that the $\epsilon_{pn} = 0$ result, which is computationally feasible for $M = 1$, is just the solution for the exact Hamiltonian H using importance sampling. A linear extrapolation of the partial node energies (green star) agrees well with the $\epsilon_{pn} = 0$ solution. (b) Partial node energies for $M = 2$, where the sign problem prevents a solution of the exact Hamiltonian. A quadratic extrapolation agrees well with the fully-signed solution (black square), which is obtained via release node QMC initialized from the ground state walkers of partial node FCI-QMC with $\epsilon_{pn} = 0.4$. (c) Average energy for 100 release node traces used in panel (b). Arrows indicate the region used in calculating statistics. Error bars show standard error across trials. The inset shows a similar release node trace in which the initial condition is intentionally far from correct, to make the decay in energy more apparent. (d) Flip rate of the denominator of the energy metric as a function of ϵ_{pn} (blue dots). For comparison, the red triangle shows the flip rate without importance sampling and the black dashed line shows the inverse of the average the Monte Carlo correlation time for our simulation. All data are for $1/(k_{FA}) = 0.9$, $\Lambda = 20k_F$, and $N = 33$. (a)-(c) use 10^6 walkers, while (d) uses 10^4 .

which we refer as the fixed node Hamiltonian without diagonal dumping – given by

$$\begin{aligned} \langle D' | H'_{\text{fn}} | D \rangle &= \begin{cases} 0 & \text{if sign viol.} \\ \langle D' | H_{\text{is}} | D \rangle & \text{if not s.v.} \end{cases}, \text{ where } D \neq D' \\ \langle D | H'_{\text{fn}} | D \rangle &= \langle D | H_{\text{is}} | D \rangle, \end{aligned} \quad (12)$$

whose ground state energy is no longer guaranteed to be a variational upper bound on that of H . In section VI we will describe the steps needed to reintroduce the upper bound.

Due to the presence of annihilation in FCI-QMC, we are able to introduce a less-severe approximation, which we call the partial node approximation. In partial node, we interpolate between the exact and fixed-node Hamiltonians

$$H_{\text{pn}} = \epsilon_{\text{pn}} H'_{\text{fn}} + (1 - \epsilon_{\text{pn}}) H_{\text{is}}. \quad (13)$$

Surprisingly, we find that this algorithm works up to a very high fraction of the original sign violating terms (small ϵ_{pn}). To obtain the exact answer, we extrapolate to the original Hamiltonian ($\epsilon_{\text{pn}} = 0$), heuristically using a quadratic fit (see fig. 3).

To quantify the improvement gained by using the partial node approximation, we measure the average flip rate of the sign of the walkers on the reference determinant D_0 (which typically should contain approximately 30% of the walkers for a given snapshot). The flipping of this sign is a signature of an instability of the algorithm coming from the sign problem, and the average flip rate must be significantly below the inverse correlation time for useful data to be garnered from the simulation. Fig. 3d shows the average flip rate using the partial node approximation. Notice that

$\epsilon_{\text{pn}} = 0$ is close to the inverse correlation time, presenting a problem, but by $\epsilon_{\text{pn}} = 0.4$ the flip rate has significantly decreased.

V. RELEASE NODE

In FCI-QMC without annihilation, the sign problem manifests as a variance that scales exponentially with both β and the energy difference between the fermionic and bosonic ground states⁶. This exponential scaling in β holds even in the presence of annihilation at finite walker number, as annihilation can be thought of as simply reducing the fermion-boson ground state gap. Therefore, minimizing the total β needed to reach the ground state wave-function with a certain fidelity also minimizes the effect of the sign problem. Thus, one can improve the convergence time of the importance-sampled FCI-QMC algorithm ($\epsilon_{\text{pn}} = 0$) by starting very close to the ground state.

One approach to starting near the true ground state is to use the ground state of H_{pn} with a small value of ϵ_{pn} . We aren't able to explicitly represent this wavefunction, but we can prepare it stochastically via partial node FCI-QMC. The set of N_w walkers thus prepared is then allowed to evolve under the true Hamiltonian for fixed imaginary time β . When the wavefunction is “released” to evolve under the exact Hamiltonian, it quickly relaxes to the exact ground state; this is what we call release-node FCI-QMC¹⁴.

In release node, we use the same energy metric as in importance sampled FCI-QMC. In this case, since we have now propagated with two non-commuting Hamiltonians (H_{pn} and H_{is}), one can show that the energy metric only becomes meaningful when the wavefunction reaches the ground state, at which point it gives the ground state energy. As seen in figure 3, the energy converges to the ground state energy before the errors blow up if we start close enough to the ground state. The release node energies agree well with the partial node extrapolation (fig. 3), which provides a check of the validity of our extrapolation.

VI. DIAGONAL DUMPING

The partial node approximation that we have discussed thus far does not give a variational upper bound on the energy, since we removed the diagonal dumping to get the fixed node Hamiltonian H'_{fn} (12). To restore the variational upper bound, we now discuss how one can put the effects of the diagonal dumping back into the partial node algorithm.

While the sum involved in diagonal dumping is in general not analytically tractable, it can be done stochastically in much the same way as off-diagonal spawning. During the diagonal create/kill step¹ we would like to stochastically apply

$$U_{\text{diag}} = 1 - \tau \langle D | H_{\text{is}} | D \rangle - \tau \sum_{D' \text{ s.v.}} \langle D' | H_{\text{is}} | D \rangle \quad (14)$$

to a walker on determinant $|D\rangle$. The first two terms can be done exactly, while the sum – denoted ΔK – can be sampled as follows.

1. From $|D\rangle$ pick another determinant $|D'\rangle$ according to some normalized probability function $p_{\text{gen}}(D'|D)$.
2. If $\langle D' | H_{\text{is}} | D \rangle$ is not sign-violating, then $\Delta K = 0$.
3. Otherwise, $\Delta K = \langle D' | H_{\text{is}} | D \rangle / p_{\text{gen}}(D'|D)$.

However, as ΔK is now potentially very large, multiplying $|D\rangle$ by weight U_{diag} has the potential to be disastrous if $U_{\text{diag}} \ll -1$. Therefore, we find it necessary when stochastically dumping the diagonal to also use the approximation

$$1 - \tau \langle D | H_{\text{is}} | D \rangle - \tau \Delta K \approx e^{-\tau(\langle D | H_{\text{is}} | D \rangle - \Delta K)} \quad (15)$$

This introduces a time step error which one must extrapolate to zero; empirically a quadratic extrapolation for $\tau < 10^{-3}$ appears to be quite effective. Partial node results with stochastic dumping of the diagonal are shown in fig. 3.

VII. RESULTS

Using partial node FCI-QMC followed by release node, we are able to determine values for the energy and quasi-particle residue of the Fermi-polaron on the BEC side of the interaction, which are shown in fig. 4 for $\Lambda = 20k_F$ and

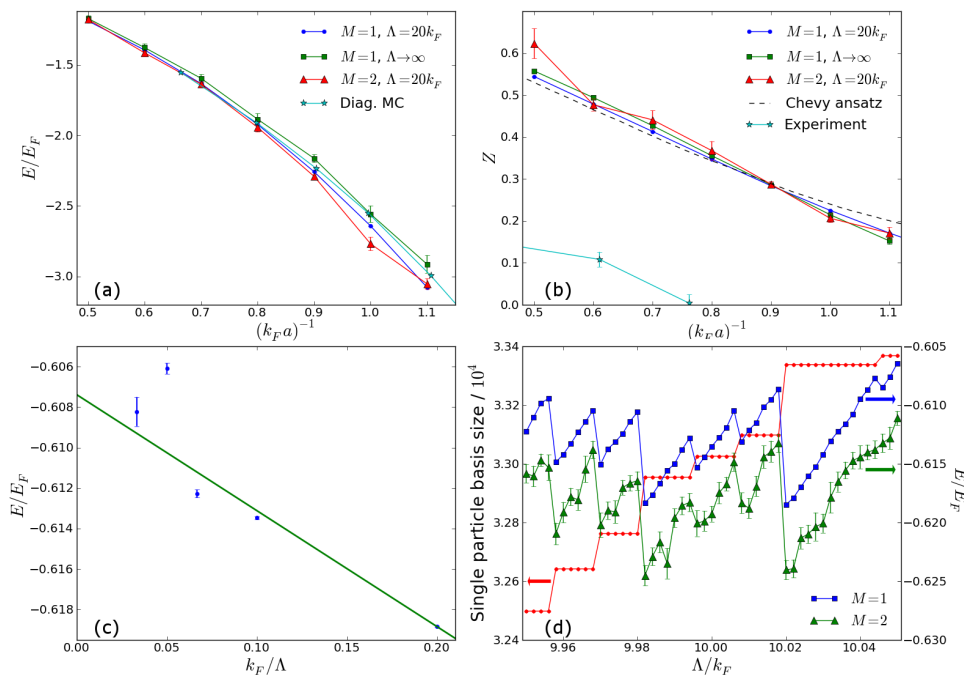


FIG. 4: (color online) Ground state energy (a) and quasiparticle residue (b) for the polaron off of unitarity at $\Lambda = 20k_F$ and $N = 33$. Energies are compared against the $N \rightarrow \infty$, $\Lambda \rightarrow \infty$ results from diagrammatic MC⁹, while Z is compared to experimental measurements⁸ and the analytical variational result at $M = 1$ ⁷. Deviations of Z from the analytic results likely come from a combination of finite size effects and error in the mixed estimator. (c) and (d) show finite size effects seen in attempting to extrapolate the energy in $1/\Lambda$, with $(k_F a)^{-1} = 0$, $N = 33$, $M = 1$ (c) and 2 (c,d). In (d), we compare energy against single particle basis size, i.e. the number of available spin up momenta $k_F < k < \Lambda$.

$N = 33$. The energies are compared to polaron and molecule energies from diagrammatic Monte Carlo⁹. Our results match well for small values of $1/(k_F a)$, while for larger values of $1/(k_F a)$ our energies deviate from the diagrammatic results. This is a consequence of working at fixed $\Lambda = 20k_F$, as opposed to diagrammatic Monte Carlo, which is done in the limit $\Lambda \rightarrow \infty$. Our results match with the diagrammatic solution after extrapolating to $\Lambda = \infty$.

Figure 4b shows the quasiparticle residue Z compared to experimental results⁸, where there is a small but finite density of spin-down atoms. We find that, as with the energy, an $M = 1$ variational expansion provides a good estimate of Z . Therefore, as noted elsewhere⁸, our theoretical model differs significantly from the experiment, possibly as a result of the finite spin-down density used experimentally.

In extrapolating our results to the physical limit, $\Lambda \rightarrow \infty$, we encountered an unexpected problem. Using a linear fit over a wide range of $1/\Lambda$ (fig. 4a), we find that individual data points have error well outside the line, with no discernible pattern. Zooming into a very small region of Λ we discovered the reason behind this: small fractional increases in basis size as new shells become available cause large jumps in the ground state energy. A similar issue occurs when attempting to extrapolate in particle number N . We nevertheless attempt such an extrapolation in fig. 4 a and b. As a result, the size of the error bars reflects not the accuracy of the data points at individual values of Λ , but rather these inherent shell effects.

Shell effects will vanish in the limit $N \rightarrow \infty$. Therefore, we next address the possibility of extending FCI-QMC into the thermodynamic limit.

VIII. FCI-QMC IN THE THERMODYNAMIC LIMIT

All the quantum Monte Carlo simulations described so far have been done for a finite number of particles. In this section, we describe how to modify FCI-QMC to work directly in the thermodynamic limit (TDL, $N \rightarrow \infty$). In the thermodynamic limit, the accessible momenta span a continuous set of k -points instead of being limited to a discrete grid. Additionally, it is important to work in a representation where instead of enumerating the momenta for all $N = \infty$ particles, we instead store only their excitations above a known state, in this case $|D_0\rangle$. Crucially, in order for the spectrum of the Hamiltonian to remain bounded, allowing application of $1 - \tau H$ instead of $e^{-\tau H}$, the TDL only works with a cutoff M on the number of excitations allowed. We note that there are modifications to FCI-QMC

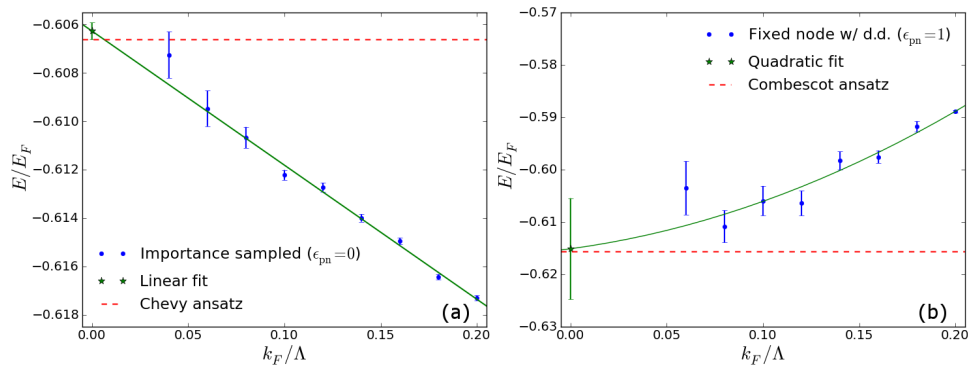


FIG. 5: (color online) Ground state polaron energy in the TDL (a) with $M = 1$, $(k_F a)^{-1} = 0$ as a function of Λ (blue dots). A linear extrapolation in $1/\Lambda$ (green star) agrees with the exact ground state energy with $M = 1$, calculated by Chevy's variational ansatz⁷. (b) Fixed node ($\epsilon_{pn} = 1$) energies for $M = 2$ compared against the variational ansatz¹⁰.

that can allow it to work in continuous time, i.e. allow for application of $e^{-\tau H}$, which we discuss in appendix A. This requirement is similar in spirit to the diagrammatic Monte Carlo method of imposing a cutoff on diagram order, in an attempt to avoid a divergence.

As momentum space is no longer discretized in the TDL, one might assume that annihilation is no longer possible, and therefore that the algorithm is doomed to fail. However, there is one key exception: due to the discrete choice of $|D_0\rangle$, annihilation can still occur at that one determinant.

Given this, the TDL algorithm is in practice nearly identical to the algorithm with finite N – in fact, one can think of the TDL algorithm as just the limit of the finite algorithm for larger and larger N . We have carefully, though implicitly, defined $|\psi_T\rangle$ such that all factors of \mathcal{V} cancel out when determining relevant quantities, such as spawning probability or energy. This is important because taking the limit $N \rightarrow \infty$ while at fixed spin-up density (constant k_F) means taking $\mathcal{V} \rightarrow \infty$ as well.

The TDL algorithm is remarkably effective at finding the ground state with $M = 1$ at unitarity, where the sign problem is weak. These energies at various values of Λ are shown in fig. 5a, where an extrapolation to $\Lambda = \infty$ is much smoother than for finite N due to the absence of shell effects.

For the sign-problem-heavy $M = 2$ case, we instead show data in the sign-free fixed node limit ($\epsilon_{pn} = 1$), using the diagonal dumping method described in sec. VI. This gives a good energy for the $M = 2$ polaron, which is a variational upper bound on the known energy of $-0.6156E_F$ within error bars. We believe this latter approach of combining fixed node with working directly in the thermodynamic limit will have wide applicability even for the approximate calculations that currently dominate the fermion QMC literature.

IX. DISCUSSION

We have shown that the FCI-QMC algorithm can solve the Fermi polaron problem, after improving the algorithm with a smart importance sampled wave function, the introduction of partial and fixed node approximations, and the utilization of release node methods.

We believe that our work demonstrates two main points that should be useful as FCI-QMC and its variants are applied to future problems in condensed matter physics. First, for strongly correlated condensed systems where many determinants are occupied in any single particle basis, we have demonstrated that physical insight – in the form of a good choice of trial wavefunction – can significantly improve the behavior of the FCI-QMC algorithm. Combining the improved statistics of importance sampling with sign-attenuating approximations such as partial node, we showed a significant increase in the effectiveness of FCI-QMC in solving the polaron problem. Finally, we showed that these methods can be made exact, up to statistical noise, via extrapolation or release node QMC.

Second, we have shown that under certain conditions the FCI-QMC algorithm can be extended to work with systems in the thermodynamic limit. Furthermore, we have introduced a fixed node algorithm in this limit, which has historically been an important tool for solving fermionic systems with QMC. We anticipate that these new developments will open a variety of problems in condensed matter physics to be approached using these new developments.

A. Acknowledgments

We would like to thank David Huse and Charles Mathy for valuable discussions. This work was supported in part by ARO Award W911NF-07-1-0464 with funds from the DARPA OLE Program. Some of the computation was performed using the Extreme Science and Engineering Discovery Environment (XSEDE), which is supported by National Science Foundation grant number OCI-1053575. Additional computational work was done on the Feynman cluster at Princeton.

-
- ¹ G. H. Booth, A. J. W. Thom, and A. Alavi, *Journal of Chemical Physics* **131**, 054106 (2009).
² D. Cleland, G. H. Booth, and A. Alavi, *Journal of Chemical Physics* **132**, 041103 (2010).
³ J. J. Shepherd, G. Booth, A. Grneis, and A. Alavi, arXiv:1109.2635v1 (2011).
⁴ J. S. Spencer, N. S. Blunt, and W. M. C. Foulkes, arXiv:1110.5479 (2011).
⁵ In practice, one actually applies $U_1 = 1 - \tau(H - S)$, where S is a tunable parameter that is used to control the number of walkers through a standard feedback process (details can be found in Booth et. al., 2009). This is really a technical point, rather than a physical one, since one could instead apply $1 - \tau H$ with occasional resampling.
⁶ M. Kolodrubetz and B. K. Clark, arXiv:1202.0525v1 (2012).
⁷ F. Chevy, *Phys. Rev. A* **74**, 063628 (2006).
⁸ A. Schirotzek, C.-H. Wu, A. Sommer, and M. W. Zwierlein, *Phys. Rev. Lett.* **102**, 230402 (2009).
⁹ N. V. Prokof'ev and B. V. Svistunov, *Phys. Rev. B* **77**, 125101 (2008).
¹⁰ R. Combescot and S. Giraud, *Phys. Rev. Lett.* **101**, 050404 (2008).
¹¹ C. J. M. Mathy, M. M. Parish, and D. A. Huse, *Phys. Rev. Lett.* **106**, 166404 (2011).
¹² D. M. Ceperley and M. H. Kalos, in *Monte Carlo Methods in Statistical Physics*, edited by K. Binder (Springer-Verlag, 1979).
¹³ H. J. M. van Bemmelen, D. F. B. ten Haaf, W. van Saarloos, J. M. J. van Leeuwen, and G. An, *Phys. Rev. Lett.* **72**, 2442 (1994).
¹⁴ D. M. Ceperley and B. Adler, *Journal of Chemical Physics* **81**, 5833 (1984).
¹⁵ S. Sorella and F. Becca, *Sissa lecture notes on numerical methods for strongly correlated electrons* (2011), URL <http://people.sissa.it/~sorella/Simulazioni.pdf>.

Appendix A: Continuous-time algorithm for FCI-QMC

In this appendix, we introduce a continuous-time FCI-QMC algorithm that has no fixed time step. We note that, while we have not yet implemented this algorithm, the number of off-diagonal terms that must be sampled to remove the penalty method errors (discussed below) is likely to make the algorithm significantly slower than the finite time step algorithms described earlier.

Our continuous-time formulation of FCI-QMC is loosely based on a continuous-time lattice algorithm found elsewhere¹⁵. We will begin by introducing the algorithm for an arbitrary Hamiltonian H , which in general can be some non-Hermitian effective Hamiltonian, as found in importance sampling. We will start by assuming that all off-diagonal sums can be computed analytically, and later generalize this to the case where certain sums must be done stochastically. We generalize the existing algorithm to allow for situations where H has a sign problem, so off-diagonal elements of H will not be required to be negative.

We would like to apply the propagator $U_{\beta_A} = e^{-\beta_A H}$, where β_A is now some fixed imaginary time. We refer to β_A as the annihilation time, and think of applying U_{β_A} to each walker before performing annihilation. Breaking this up into small time intervals τ , it becomes $U_{\beta_A} = (1 - \tau H)(1 - \tau H) \cdots (1 - \tau H)$. To perform continuous time QMC, we would like to take the $\tau \rightarrow 0$ limit of this expression.

Consider applying $U_\tau = 1 - \tau H$ stochastically to some determinant $|D\rangle$ in the limit $\tau \rightarrow 0$. We define on-diagonal component $K_L(D)$ and off-diagonal sum $V_L(D)$, where

$$\begin{aligned} K_L(D) &= \langle D|H|D\rangle \\ V_L(D) &= \sum_{D' \neq D} |\langle D'|H|D\rangle|. \end{aligned} \tag{A1}$$

We can break U_1 up as

$$U_1 = \frac{1 - \tau K}{1 - p_s} (1 - p_s) + \frac{-\tau V}{p_s} p_s = K_1(1 - p_s) + V_1 p_s, \text{ where}$$

$$K_1 \equiv \frac{1 - \tau K}{1 - p_s} \quad \text{and} \quad V_1 \equiv \frac{-\tau V}{p_s} \quad (\text{A2})$$

Then we stochastically apply K_1 with probability $1 - p_s$ or V_1 with probability p_s .

Furthermore, we would like to choose p_s such that V_1 simply corresponds to deterministically moving to $|D'\rangle$ with probability proportional to $|\langle D'|H|D\rangle|$. Thus,

$$\sum_{D' \neq D} |\langle D'|V_1|D\rangle| = 1 \implies p_s = \tau V_L(D). \quad (\text{A3})$$

So the algorithm proceeds as follows: start from some determinant $|D\rangle$, and either apply K_1 with probability $1 - p_s$ or V_1 with probability p_s . V_1 corresponds to hopping to a new determinant. K_1 simply multiplies $|D\rangle$ by a weight

$$W_1 = \frac{1 - \tau K_L(D)}{1 - p_s} = \frac{1 - \tau K_L(D)}{1 - \tau V_L(D)}. \quad (\text{A4})$$

V_1 is chosen for the first time at step N with probability $P(N|D) = (1 - p_s(D))^N$. If $N = \beta_S/\tau$, time β_S prior to spawning will come from the probability distribution

$$P_s(\beta_S) = (1 - \tau V_L)^{\beta_S/\tau} \xrightarrow{\tau \rightarrow 0} e^{-\beta_S V_L(D)}. \quad (\text{A5})$$

Given a choice of β_S from this distribution, the walker will also pick up a total weight W during the $N - 1$ non-spawning steps, where

$$W(\beta_S) = W_1^{\beta_S/\tau - 1} \xrightarrow{\tau \rightarrow 0} e^{-\beta_S [K_L(D) - V_L(D)]} \quad (\text{A6})$$

Note that, for a non-sign-violating Hamiltonian, the term in the exponent of $W(\beta_S)$ is just the local energy.

Therefore, for each walker we stochastically propagate for a time β_A , during which it will both hop and pick up weight; this can be done to all the walkers in parallel. Finally, we take all the walkers, perform annihilation, measure observables, and repeat. For Hamiltonians with relatively few off-diagonal terms, i.e. the real-space Hubbard model, this is the complete algorithm. For much larger off-diagonal sums, things become more complicated.

The remainder of this discussion will describe our algorithm for Hamiltonians with large or infinite number of off-diagonal terms in the sums. There are two sums (integrals in the TDL) that we now perform stochastically: the diagonal dumping

$$\Delta K_L(D) = \epsilon_{\text{pn}} \sum_{D' \text{ s.v.}} |\langle D'|H_{\text{is}}|D\rangle| \quad (\text{A7})$$

and the local potential energy sum

$$V_L(D) = \sum_{D' \text{ n.s.v.}} |\langle D'|H_{\text{is}}|D\rangle| + (1 - \epsilon_{\text{pn}}) \sum_{D' \text{ s.v.}} |\langle D'|H_{\text{is}}|D\rangle|. \quad (\text{A8})$$

The sums themselves are fairly straightforward. Using the same method as spawning in FCI-QMC, we have a method for generating determinant $|D'\rangle$ connected by an off-diagonal component of H to the starting determinant $|D\rangle$. If the probability to generate $|D'\rangle$ is $p_{\text{gen}}(D'|D)$, then ΔK_L for example is just the expectation of the observable

$$\mathcal{O}_{\Delta K_L} = \epsilon_{\text{pn}} \frac{\eta_{DD'} \langle D'|H|D\rangle}{p_{\text{gen}}(D'|D)} \quad \text{where} \quad \eta_{DD'} = \begin{cases} 0 & \text{if not sign viol.} \\ 1 & \text{if sign viol.} \end{cases} \quad (\text{A9})$$

A similar observable \mathcal{O}_{V_L} can be defined for computing $V_L(D)$. Assume that we have sampled a total of N_{sum} determinants D' to simultaneously calculate ΔK_L and V_L with some mean $\bar{\mathcal{O}}$ and standard error $\sigma(\mathcal{O})$ for each observable.

Formally, we could perform this sampling in the limit $N_{\text{sum}} \rightarrow \infty$, determine ΔK_L and V_L exactly, and simply use them in the earlier procedure. However, for finite N_{sum} , we want to utilize a variant of the penalty method to minimize the bias due to statistical uncertainty. Consider first the simpler case of applying the weight $W = e^{-\beta_S \Delta K_L}$. Assume that the actual value of ΔK_L is drawn from a Gaussian distribution with mean μ and width σ , which are given by the expectation value and standard error of $\mathcal{O}_{\Delta K_L}$. Then the weight we should apply is simply

$$W_{\text{stoch}}(\Delta K_L) \equiv \langle W \rangle = \int_{-\infty}^{\infty} e^{-\beta_S \Delta K_L} G_{\mu, \sigma}(\Delta K_L) d(\Delta K_L) = e^{-\beta_S (\mu - \beta_S \sigma^2/2)} \quad (\text{A10})$$

A more complicated question is how to sample β_S in an unbiased way. Again, assume that V_L is drawn from a Gaussian $G_{\mu,\sigma}(V_L)$. Furthermore, assume that we have chosen N_{sum} large enough that we don't have to worry about the negative V_L tail of the Gaussian, i.e. $\mu \gg \sigma$. We want to sample from the full distribution

$$p(\beta_S) = \int_0^\infty p(\beta_S|V_L)G_{\mu\sigma}(V_L)dV_L \quad (\text{A11})$$

We can expand to second order in $V_L - \mu$, ignoring the first order term (whose integral vanishes). Then

$$p(\beta_S) \propto \frac{e^{-\beta_S\mu}}{\mu} \int_{-\infty}^\infty \left[1 + \left(\frac{V_L - \mu}{\mu} \right)^2 (1 + \beta\mu + \beta^2\mu^2/2) + O\left(\left(\frac{V_L - \mu}{\mu} \right)^4 \right) \right] G_{\mu\sigma}(V_L)dV_L \quad (\text{A12})$$

$$\approx \frac{e^{-\beta_S\mu}}{\mu} \left[1 + \left(\frac{\sigma}{\mu} \right)^2 (1 + \beta\mu + \beta^2\mu^2/2) \right] \quad (\text{A13})$$

Normalizing and integrating this result, we find that the normalized cumulative distribution function is

$$P(x = \mu\beta_S, s = \sigma/\mu) = 1 + \frac{(\sinh x - \cosh x)(2 + s^2(x^2 + 4x + 6))}{6s^2 + 2} \quad (\text{A14})$$

We can then sample from this distribution by picking $z \in [0, 1]$ at random, then finding the value of β_S where $P(x, s) = z$.

In summary, here is our algorithm for continuous partial node FCI-QMC:

1. Start with N_w walkers, each with weight $W_w = 1$, sign S_w , and determinant $|D_w\rangle$. At the first step, all walkers are initialized in $|D_0\rangle$ with positive sign. At this point, there should be no walkers with the same determinant but opposite sign.
2. Propagate each walker independently by $e^{-\beta_A(H-S)}$ as follows. At the start of this portion, define a variable β_w for each walker, and initialize $\beta_w = 0$.
 - (a) For a walker in determinant $|D\rangle$, sample off-diagonal elements $|D'\rangle$ for N_{sum} steps to get $\overline{V_L(D)}$, $\sigma[V_L(D)]$, $\overline{\Delta K_L(D)}$, and $\sigma[\Delta K_L(D)]$.
 - (b) Sample β_S from $P(x, s)$ as described above, where $x = \beta_S/\overline{V_L(D)}$ and $s = \sigma[V_L(D)]/\overline{V_L(D)}$.
 - (c) If $\beta_w + \beta_S < \beta_A$, then move the walker to a new determinant $|D'\rangle$. To sample with weight proportional to $|\langle D'|H|D\rangle|$, run a Metropolis algorithm for N_{met} steps. The sign of $|D\rangle$ is (not) flipped when the matrix element $\langle D'|H|D\rangle$ is positive (negative).
 - (d) Multiply the weight by $e^{-\beta_S(\langle D|H|D\rangle - S)}$, with the stochastic portion of $e^{-\beta_S\langle D|H|D\rangle}$ re-weighted via the penalty method as described above. If $\beta_w + \beta_S > \beta_A$, then use $\beta_A - \beta_w$ in place of β_S in these formulas.
 - (e) Increment β_w by β_S . If $\beta_w < \beta_A$, repeat from part (a).
3. Annihilate the walkers, keeping track of their weights. For example, if five walkers are all on determinant D with weights W_1 to W_5 and signs S_1 to S_5 , let $\widetilde{W} = \sum_i W_i S_i$. Then the five walkers are replaced by a single walker with weight $|\widetilde{W}|$ and sign $\text{sgn}(\widetilde{W})$.
4. Resample the walkers. Replace a single walker with weight W by $[W]$ walkers of weight 1. Add another walker of weight 1 with probability $W - [W]$.
5. Measure observables.
6. Adjust S using standard feedback protocols¹ as desired. Then repeat from step 1.